DNA Repair 95 (2020) 102949

Contents lists available at ScienceDirect

DNA Repair

journal homepage: www.elsevier.com/locate/dnarepair

Effects of radiotherapy and short-term starvation combination on metastatic and non-tumor cell lines

Sara Pignatta [a,*], Michela Cortesi [a], Chiara Arienti [a], Michele Zanoni [a], Claudia Cocchi [a], Anna Sarnelli [b], Donatella Arpa [c], Filippo Piccinini [d], Anna Tesei [a,*]

[a] Biosciences Laboratory, Istituto Scientifico Romagnolo per lo Studio e la Cura dei Tumori (IRST), IRCCS, Meldola, Italy
[b] Medical Physics Unit, Istituto Scientifico Romagnolo per lo Studio e la Cura dei Tumori (IRST) IRCCS, Meldola, Italy
[c] Radiotherapy Unit, Istituto Scientifico Romagnolo per lo Studio e la Cura dei Tumori (IRST) IRCCS, Meldola, Italy
[d] Scientific Directorate, Istituto Scientifico Romagnolo per lo Studio e la Cura dei Tumori (IRST) IRCCS, Meldola, Italy

ARTICLE INFO

Keywords:
Radiotherapy
Short-term starvation
Dietary restriction
Radiobiology
Differential stress resistance
DNA damage

ABSTRACT

Background: Since its discovery in the late 19th century, radiotherapy has been one of the most important medical treatments in oncology. Recently, fasting or short-term starvation (STS) in cancer patients undergoing chemotherapy has been studied to determine its potential for enhancing the therapeutic index and for preventing side-effects, but no data are available in the radiotherapy setting. We thus decided to investigate the effects *in vitro* of STS in combination with radiotherapy in metastatic cancer cells and non-cancer cells.
Methods: Cells were incubated in short-term starvation medium (STS medium, 0·5 g/L glucose + 1% FBS) or in control medium (CM medium, 1 g/L glucose + 10 % FBS) for 24 h and then treated with single high-dose radiation. A plexiglass custom-built phantom was used to irradiate cells. DNA damage was evaluated using alkaline comet assay and the*CometAnalyser* software. The cell surviving fraction was assessed by clonogenic assay.
Finding: STS followed by single high-dose radiation significantly increased DNA damage in metastatic cancer cell lines but not in normal cells. Furthermore, STS reduced the surviving fraction of irradiated tumor cells, indicating a good radio-sensitizing effect on metastatic cell lines. This effect was not observed in non-tumor cells.
Interpretation: Our results suggest that STS may alter cellular processes, enhancing the efficacy of radiotherapy in metastatic cancer cells*in vitro*. Interestingly, STS has radioprotective effect on the survival of healthy cells.

1. Introduction

Radiotherapy (RT) is one of the major medical treatments in oncology, used in both adjuvant and palliative care settings, and contributes to improve patient overall survival. In recent years, great efforts have been made to improve RT. There has been substantial progress in several areas such as dose delivery, prescription and distribution, and also in the development of new technologies for image guidance [1].

The use of high-dose single fraction therapy for the control of local disease and metastases has obtained increasingly impressive results. Several studies using single-dose or up to three large fractions of radiotherapy have been performed for lung, kidney, pancreatic cancer, liver, brain, and spine metastases, demonstrating improved disease control [2–4]. However, the identification of strategies to selectively increase tumor cell radio-sensitivity and normal cell radio-resistance is needed to further improve RT outcome.

Preclinical studies have shown that fasting and calorie restriction in combination with chemotherapy could have potential for clinical development. There is also evidence to suggest that this combination could enhance therapeutic index and lessen the side-effects of chemotherapy [5]. Moreover, several authors have reported that nutrient modulation through diet, fasting or short-term starvation (STS) can selectively protect normal cells in mice [6,7] and, potentially, in patients from chemotoxicity, without reducing the therapeutic outcome on cancer cells [2,8,9]. This phenomenon was first described by Sadfie et al. [10] as differential stress resistance (DSR) and is based on the hypothesis that normal cells change their metabolic state during STS, redistributing cellular energy from a reproduction/growth program to one of protection/maintenance. Conversely, cancer cells characterized by a constitutive activation of proliferative pathways caused by mutations in

* Corresponding authors at: Biosciences Laboratory, Istituto Scientifico Romagnolo per lo Studio e la Cura dei Tumori (IRST), IRCCS, Via P. Maroncelli 40, 47014 Meldola, Italy.
E-mail addresses: sara.pignatta@irst.emr.it (S. Pignatta), anna.tesei@irst.emr.it (A. Tesei).

https://doi.org/10.1016/j.dnarep.2020.102949
Received 30 March 2020; Received in revised form 22 July 2020; Accepted 8 August 2020
Available online 16 August 2020

oncogenes and tumor suppressor genes, are unresponsive to DSR [11, 12].

In addition to the extraordinary advances made in the field of oncology, researchers have recently elucidated the biochemical bases and metabolic pathways of some hallmarks of cancer, including sustained proliferation signaling, growth suppressor evasion, and cell death resistance [13]. It is known that cancer-altered metabolism boosts the adoption of compensatory pathways to generate energy in malignant cells. Furthermore, cancer cells are characterized by mutations in oncogenes such as IGF-1 receptor (IGF-1R), GTP proteins RAS/RAF, mitogen-activated protein kinase (MAPK), phosphatidylinositol 3-kinase (PI3K), and c-Myc transcription factor, all of which coordinate cell progression and proliferation independently, or almost independently, of external growth factors [2,14–16]. They also show insensitivity to inhibitory signals due to loss-of-function mutations in tumor suppressor genes, *e.g.* p53, p21 and PTEN [17].

The loss-of-function or mutations in genes involved in DNA repair appear to be associated with variations in sensitivity to radiation therapy. In particular, the dysregulation of cell cycle arrest is a key event in radiation response. G1/S and G2/M checkpoints are activated to allow DNA repair and impairments of this mechanism cause an accumulation of DNA damage. Consequently, the modulation of cell cycle kinetics induced by diets or food intake in both normal and cancer cells may lead to divergent DNA repair and a different response to RT [18]. In addition, factors other than diet may affect cancer cell metabolism. It is worthy of note that the rate of glycolysis is enhanced under hypoxic conditions, resulting in increased lactate levels. The expression of hypoxia-inducible transcription factors 1a (HIF-1a) and 2a (HIF-2a), cause the upregulation of glucose transporters and glycolytic enzymes, promote the expression of stem cell gene, and influence tumor radiosensitivity [19, 20]. We therefore hypothesized that short-term starvation could be a useful adjuvant for radiotherapy treatment.

In the present work we evaluated the potential of short-term starvation (STS) combined with RT to increase the efficacy of radiation treatment in metastatic cancer cells, whilst also protecting normal cells. We focused on high-dose single-fraction radiotherapy and used cell lines derived from prostate cancer spinal lesions and from pancreatic cancer liver metastases. High-dose radiation for spinal metastases and pancreatic tumors delivered in a small number of fractions over 5–10 days could be an ideal setting to combine with starvation or fasting, making a 24 -h fasting more tolerable for the patient than conventional fractionation regimens, characterized by daily radiotherapy sessions.

2. Material and methods

2.1. Cell lines

MRC-5 (normal fibroblast lung cell line; RRID:CVCL_0440), VCaP (prostate cancer cell derived from vertebral metastasis; RRID: CVCL_2235), CFPAC-1 (pancreatic cancer cell derived from liver metastasis; RRID:CVCL_1119), HUVEC (human umbilical vein endothelial cells) and THP-1 (RRID:CVCL_0006) were obtained from the American Type Culture Collection (ATCC, Rockville, MD). MRC-5, VCaP, CFPAC-1 and HUVEC were maintained in DMEM (glucose 1 g/L) (Euroclone, Milan, Italy) supplemented with 10 % fetal bovine serum (Euroclone, Milan, Italy) and 1% L-glutamine (Euroclone, Milan, Italy) at 37 °C in 4% O2 under hypoxic conditions. For experiments, HUVEC were used within 24 h after reaching confluence, between passages 3 and 10. THP-1 were maintained in RPMI-1640 medium supplemented with 10 % heat-inactivated fetal bovine serum (Euroclone, Milan, Italy), 1% L-glutamine (Euroclone, Milan, Italy) 100 U/mL penicillin (Thermo Fisher Scientific, Italy) and 100 µg/mL streptomycin (Thermo Fisher Scientific, Italy). The culture was maintained at 37 °C in a humidified atmosphere containing 5% CO2.

2.2. Treatments

STS treatments. Glucose restriction was performed by maintaining cells in Gibco glucose-free DMEM (Thermo Fisher Scientific, Italy) supplemented with either low glucose (0·5 g/L) and 1% fetal bovine serum for 24 h [12].

Radiation exposure. Monolayer cell cultures in 96-well plates or in flasks were inserted into a custom built plexiglass phantom and irradiated using the linear acceleration Elekta Synergy Platform system, as previously described [21]. Cell lines were maintained in STS medium for 24 h and were then irradiated. The delivery dose used was 5 Gy for the normal fibroblast lung cell line, 8 Gy for VCAP, and 10 Gy for CFPAC-1. The radiation plan was chosen on the bases of organ dose and clinical treatment. Endotelial cells (HUVEC) and Thp1 were irradiated with all treatment plans.

2.3. Cell viability analysis

The cell viability assay was performed with CellTiterGlo™ (Promega, Milan, Italy) according to the manufacturer's instructions. Briefly, 5000 cells were cultured in a 96-well plate and 100 µL of reconstituted CellTiter-Glo reagent was added to each well. The plate was mixed on an orbital shaker for 2 min to induce cell lysis and incubated for 10 min at room temperature. The luminescent signal was recorded using Glomax (Promega, Milan, Italy).

2.4. In vitro glucose uptake activity

Glucose uptake was measured with the Glucose Uptake-Glo™ Assay (Promega, Milan, Italy) according to the manufacturer's instructions. Briefly, cells stimulated or not with STS were washed with PBS-1X and incubated with 2DG for 10 min. Stop buffer, neutralization buffer, and the detection reagent were added. The luminescence signal was recorded after 2 -h incubation.

2.5. Clonogenic assay

Clonogenic assay was performed as previously described [22]. Briefly, following treatment, 500 cells were seeded in 10 cm^2 dishes in 500 mL of medium. After 15 days, the resulting colonies were fixed and stained using 0.5 % crystal violet in 25 % methanol. Colonies with more than 50 cells were quantified under inverted microscope (I500X, Olympus) by two independent observers. Five series of samples were prepared for each treatment dose.

2.6. Flow cytometry

Flow cytometric acquisitions were performed using a FACS Canto flow cytometer (Becton Dickinson, San Diego, CA) as previously described [23]. Data were analyzed by FACSDiva software (Becton Dickinson, San Diego, CA) and ModFit 2.0 (DNA Modelling System, Verity Software House, Inc., Topsham, ME). Samples were run in triplicate and 10,000 events were collected for each replica. Data were the average of three experiments.

Cell cycle distribution. After each treatment, cells were harvested and fixed in 70 % ethanol and stored at 4 °C overnight. The fixed cells were centrifuged at 1000×*g* for 5 min and washed with cold phosphate-buffered saline (PBS). Cells were then stained with propidium iodide (10 mg/mL, MP Biomedicals, Verona, Italy), RNAse (10 kunits/mL, Sigma Aldrich) and NP40 (0·01 %, Sigma Aldrich) overnight at 37 °C in the dark and analyzed by flow cytometry. Data were expressed as fractions of cells in the different cycle phases.

γH2AX detection. After each treatment, cells were fixed in 4% paraformaldehyde and 70 % ethanol. The fixed cells were resuspended in permeabilization solution (0.1 % Triton-X100, in PBS) for 10 min at room temperature, blocked, and incubated in primary antibody (anti-

phospho-γH2AX 1:250, Millipore Cat# 16–193, RRID:AB_310795) for one hour at 4 °C, washed and incubated with fluorochrome-conjugated secondary antibodies (anti-Mouse Alexa Fluor 488 conjugate 1:250, Thermo Fisher Scientific Cat# A-11,001). Cells were then stained with propidium iodide as described above.

2.7. Immunofluorescence staining

Cells were harvested by trypsinization, washed with serum and PBS1X and plated onto glass coverslips. The cells were fixed with paraformaldehyde for 15 min on ice. The coverslips were incubated overnight at 4 °C in primary antibody (anti Rad51 1:250 Millipore Cat# ABE257, RRID:AB_10850319 ; anti-phospho-γH2AX 1:100, Millipore Cat# 16–193, RRID:AB_310795), diluted in blocking buffer, and then washed again with PBS1X and incubated with fluorochrome-conjugated secondary antibodies (anti-Rabbit Alexa Fluor 488 conjugate 1:250, Thermo Fisher Scientific Cat# A-11034, RRID:AB_2576217; anti-Mouse Alexa Fluor 488 conjugate 1:250, Thermo Fisher Scientific Cat# A-11,001, RRID:AB_2534069) for 2 h at room temperature. Cells were analyzed with Nikon A1 confocal laser scanning microscope equipped with a 60×, 1.4 NA objective and with 405 and 488 nm laser lines. A minimum of 100 cells were analyzed for each condition and the cells containing a minimum of 5 RAD51 and γH2AX foci per nucleus were scored as positive. Automatic focus scoring was performed using the cell image analysis software, Fiji ImageJ. All image analysis parameters were kept constant throughout the duration of the experiments.

2.8. Comet assay

The alkaline comet assay was performed according to the manufacturer's protocol (Comet assay, Trevigen, Gaithersburg, MD). Briefly, at the end of the treatments, 5000 cells were suspended in LMAgarose at 37 °C and immediately transferred onto the comet slide. The slides were immersed for one hour at 4 °C in a lysis solution, washed in the dark for one hour at room temperature in an alkaline solution, and electrophoresed for 30 min at 21 V. Slides were then dipped in 70 % ethanol and stained with the Syber green (Bio-Rad Laboratories, Hercules, CA, USA). One hundred comets from category 0 to category 4 were selected and images were captured using an EVOS microscope (Thermo Fisher Scientific) at 10x magnification.

DNA damage was quantified in single cells by computing the displacement between the genetic material contained in the nucleus (comet head) and the genetic material in the surrounding part (comet tail). In order to obtain reproducible and reliable quantitative data, we used a software tool called *CometAnalyser*.

CometAnalyser is a homemade tool developed with the goal to be extremely user friendly. It can be used for the analysis of both fluorescent and silver-stained images. The working procedure has 3 main steps. (*a*) The user draws with the mouse a region surrounding the cells of interest. The tool then automatically segments comet heads and nuclei by analyzing the local histogram of the intensity values. The Otsu thresholding segmentation method is used by default [24], but other algorithms are available and several parameters can be then modified to adjust the segmentation. (*b*) Once the comets have been segmented, the tail moment and all the other morphological features listed by Gyori et al. [25] are automatically computed and saved as an *Excel* file. (*c*) Finally, the snapshots of all the segmented comets are stored in different folders according to a classification manually defined by the user. *CometAnalyser* was developed in *MatLab* (The MathWorks, Inc., Natick, MA, USA) and the current version (*i.e., CometAnalyser* v0.9) requires *MatLab R2017b* and the *MatLab Image Processing Toolbox 10.1*, or a later version. A *Windows 64-bit* standalone executable version (*i.e.,* not requiring *MatLab* being installed in the computer) of the tool is available on request.

2.9. Real-time quantitative polymerase chain reaction (RT-qPCR)

Total RNA was extracted from cell lines using TRIzol® reagent following the manufacturer's instructions (Invitrogen, Carlsbad, USA). Reverse transcription (RT) reactions were performed in 20-μL volume containing 400 ng of total RNA using an iScript TM cDNA Synthesis kit (Bio-Rad Laboratories, Hercules, CA, USA). mRNA levels of the selected genes were assessed by real-time quantitative PCR (RT-qPCR) using costum TaqMan probes (Applied Biosystems, Carlsbad, CA) and an ABI7500 system. Probes were selected from inventoried gene expression assays (Invitrogen, Thermo Scientific). The comparative threshold cycle (Ct) method was used to calculate the relative gene expression. Gene target expression was normalized to the endogenous reference genes, beta-actin and HPRT. M1/M2 polarization genes expression was normalized to endogenous reference gene RSP6. Reference genes were chosen using the geNorm VBA applet for Microsoft Excel to determine the most stable reference genes. Relative quantification of target gene expression was calculated using the comparative Ct method. The TaqMan assay used are listed in Table S1. All experiments were performed in triplicate.

2.10. Angiogenesis experiments

Angiogenesis assay was performed using *in vitro* angiogenesis kit (Abcam; cat# AB204726) following the manufacturer's instructions. In brief, ECM gel solution was added to a 96-well plate and solidified at 37 °C for 20 min. 5×10^4 cells were seeded to each well and cultured for 10 days after radiotherapy treatment. Tube formation was analyzed using Angiogenesis Analyser (Fiji ImageJ software).

2.11. THP-1 macrophage differentiation and polarization

THP-1 monocytes were differentiated into resting macrophages (M0) using 100 nM phorbol 12-myristate 13-acetate (PMA, Sigma-Aldrich) for 24 h in control medium or in STS medium. M0 macrophages were exposed to ionizing radiation and after 48 h M1/M2 gene expression panel was determined.

2.12. Statistical analysis

Experiments were performed in triplicate and results are expressed as mean ± standard deviation (SD). The Student-*t* test was used to compare the 2 groups. Data obtained from quantitative Real-Time PCR experiments were analyzed by comparing groups of mean values using one-way ANOVA with Tukey's multiple comparison test. Data were processed using the GrafPad Prism program (version 4) (GraphPad Software, San Diego California USA). A p value $<0{\cdot}05$ was considered statistically significant.

3. Results

3.1. Cell viability of starved and non-starved irradiated cell lines and impact on cell cycle phases

As a first step, a cell viability assay was performed to establish the effect of radiation in cells grown in control medium (CM) or STS medium. The radiation dose was chosen basing on clinical treatments.

Radiation caused 50 % of cell death in MRC-5 and 35 % in VCaP cell lines (Fig. 1a). Moreover, the difference in viability between cells treated with radiation alone or combined with STS were not significant ($P \geq 0{\cdot}05$), indicating that STS had no effect on the cell death rate after 72 h.

The metastatic pancreatic cell line (CFPAC-1) proved to be the most radiosensitive cell line, displaying a 90 % cell death rate after radiation treatment. Furthermore, the combination of RT and STS induced a significant inhibition of cell viability ($P < 0{\cdot}05$) with respect to RT alone

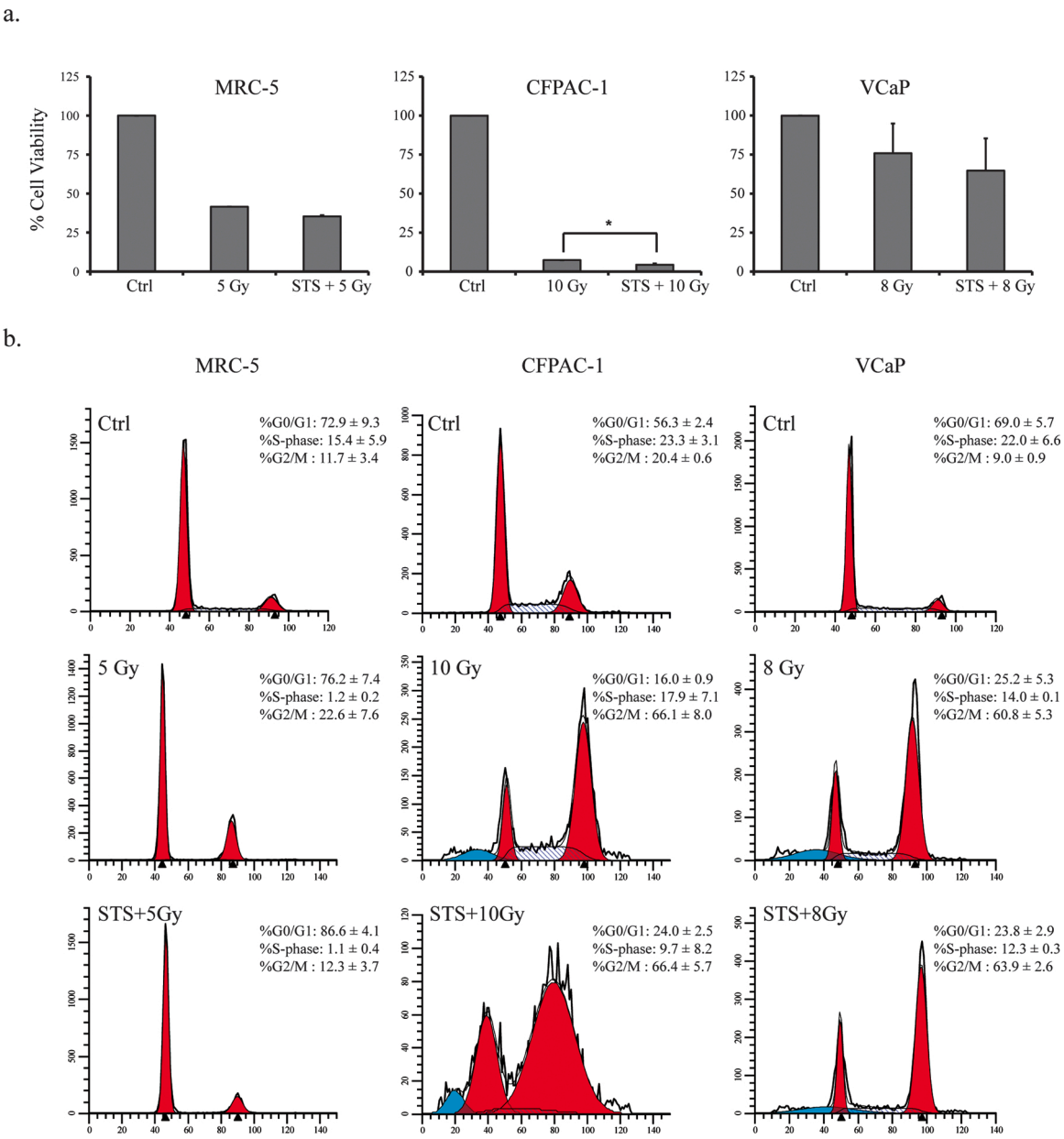

Fig. 1. Effect of RT on cell viability and cell cycle. (a) MRC-5, CFPAC-1 and VCaP cell lines were exposed to ionizing radiation (IR) in normal medium (CM) or in short-term starvation medium (STS). Cell viability was evaluated using the CellTiter-Glo™ assay 72- hour after the end of IR. Data are reported as the mean ± SD for three separate experiments performed in octuplicate. (*$p <$ 0·05). (b) Cells were exposed to STS or CM medium for 24 h and then treated with RT. Cell cycle was analyzed after 72 h by flow cytometry. The percentage of cells in each cell cycle phase represents the mean ± SD for three independent experiments.

(Fig. 1a).

RT prevents cell growth, proliferation and DNA synthesis and is known to be more effective when delivered during the appropriate cell cycle phases. We thus performed cell cycle analysis to see whether RT affected cell cycle arrest, observing that RT induced a decrease in S-phase population and an increase in G2/M phase in MRC5 cell line. RT in combination with STS resulted in an increase in G0/G1 phase and a reduction in G2/M phase with respect to RT alone (Fig. 1b). Conversely, a different distribution of cells in cycle phases was observed in both metastatic cell lines after RT treatment, characterized by a drop-off in the G0/G1 population associated with an increase in G2/M phase (Fig. 1b). The synergistic effect of the combination was seen in the CFPAC-1 cell line, suggesting that a cell-cycle-controlled regimen, such as STS followed by irradiation, could be very effective for some types of cell lines.

3.2. STS enhances the radiosensitivity of metastatic cancer cells

An initially curative treatment in cancer patients is often followed by re-growth of the tumor due to a small number of cells that retain colony-forming ability and is associated with poor clinical outcome. We performed colony formation assays to evaluate the long-term response and colony forming ability of the different cell lines to RT alone and to the STS + RT combination. Cells were incubated in STS or CM for 24 h, treated with a single dose of irradiation and fixed after 15 days (Fig. 2a). The surviving fraction of MRC-5 was significantly enhanced by the combination, suggesting that STS may protect normal tissue from RT damage (Fig. 2b).

STS for 24 h before RT caused a significant radiosensitizing effect in metastatic cell lines CFPAC-1 and VCaP (Fig. 2c–d), with complete inhibition of proliferation potential in VCaP. Furthermore, we observed a significant reduction in colony-forming ability in starved VCaP cells

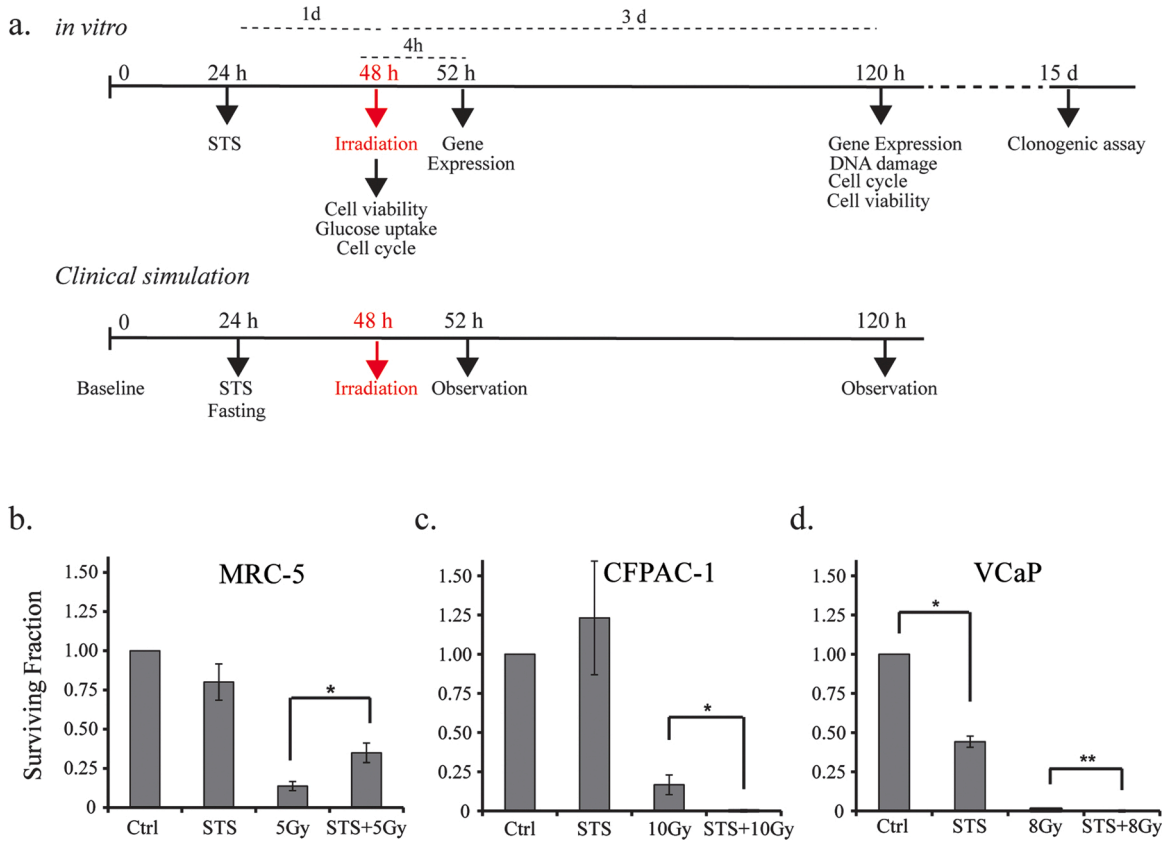

Fig. 2. Timeline of the experiments and clonogenic assay. (a) Schematic timeline and design of the experiments *in vitro* and timing simulation *in vivo*. (b) The surviving fraction was analyzed for cell lines treated with RT in CM or STS medium. Data are reported as the mean values (±SD) from three independent experiments. Statistical significance $*p < 0{\cdot}05$, $**p < 0{\cdot}01$.

with respect to control (Fig. 2d).

3.3. DNA damage increasing in starved-irradiated cancer cells

We hypothesized that STS conditions may enhance RT sensitivity by increasing DNA damage in irradiated cancer cells. To test this hypothesis, we performed alkaline comet assay to determine the radioresponsiveness of normal and metastatic cell lines in association with STS. The amount of DNA damage in irradiated MRC-5 cells was reduced when RT was combined with STS, suggesting a protective role of STS (Fig. 3). Conversely, a comparison of %tail DNA between irradiated fractions revealed a significant 2-fold or more increase in DNA damage in starved-irradiated CFPAC-1, and 0·25-fold increase in VCaP (Fig. 3b).

In metastatic cancer cells, STS conditions determined an increase of % tail DNA with respect to control, contrariwise in MRC-5 this phenomenon was not observed (Fig. 3b).

We classified comets into 5 categories on the basis of % tail DNA, ranging from class 0 (undamaged) to class 4 (maximally damaged). In MRC-5, we observed a higher number of comets in class 0 and class 1 in starved-irradiated cells than in those treated with RT alone. Conversely, STS conditions in all metastatic cell lines led to fewer comets in class 0 and a higher number of comets in classes 3 and 4 in irradiated cells than in cells treated with RT alone (Fig. 3c).

We observed in CFPAC-1 and VCaP a greater number of comets in class 2 in STS alone with respect to MRC5, in this cell line on the other hand we determined an increase of comet in class 1 (Fig. 3c).

Overall, these results strongly support previous observations that STS may increase the radiation therapeutic index in metastatic cancer cell lines and may protect normal cells from radiation damage.

γ-H2AX phosphorylation is involved in the response to DNA damage indicating the formation of DNA double-strand breaks and also in response to DNA replication stress. We evaluated the damage induced by RT and STS + RT by performing parallel qualitative and quantitative using flow cytometry (Fig.S1a) and using microscopy analyses of phosphorylate histone H2AX foci (γH2AX) in cell nuclei (Fig. 4a). Co-staining for phosphorilated- γH2AX and DNA content (propidium iodide) indicate a significative increase of H2AX phosphorylation in metastatic cancer cell lines with a percentage positive cells of about 5% in respect to control. Conversely, starved MRC-5 cells showed unchanged basal level of γ -H2AX positive cells with respect to MRC-5 cultivated in normal medium (Fig.S1a). In microscopy analysis, the number of foci increased in irradiated MRC-5 cells but substantially decreased in the same cells treated with the STS + RT combination. High numbers of foci were detected in CFPAC-1 and VCaP. Interestingly, STS pre-treatment before RT resulted in a 2-fold increase in γ -H2AX foci with respect to RT alone. Cells were also stained with RAD51, which accumulates at sites of broken DNA (Fig. 4b). The number of RAD51 foci present in MRC-5 cells treated with RT alone was indicative of considerable DNA damage, denoting a protective role of STS + RT. CFPAC-1 cells exhibited DNA damage accumulation, with an increase in RAD51-positive cells after ionizing radiation. However, a virtually identical response was observed between cells treated with RT and those undergoing the RT + STS combination. In VCaP cell line RAD51expression was localized to cytoplasm. The number of nuclear foci was not determined.

3.4. Gene expression after short-term starvation and RT treatment

To better understand the mechanism by which RT is more effective when combined with STS in metastatic cells, we hypothesized that low glucose levels may be responsible for the activation or inactivation of genes involved in the DNA damage repair machine. We thus decided to

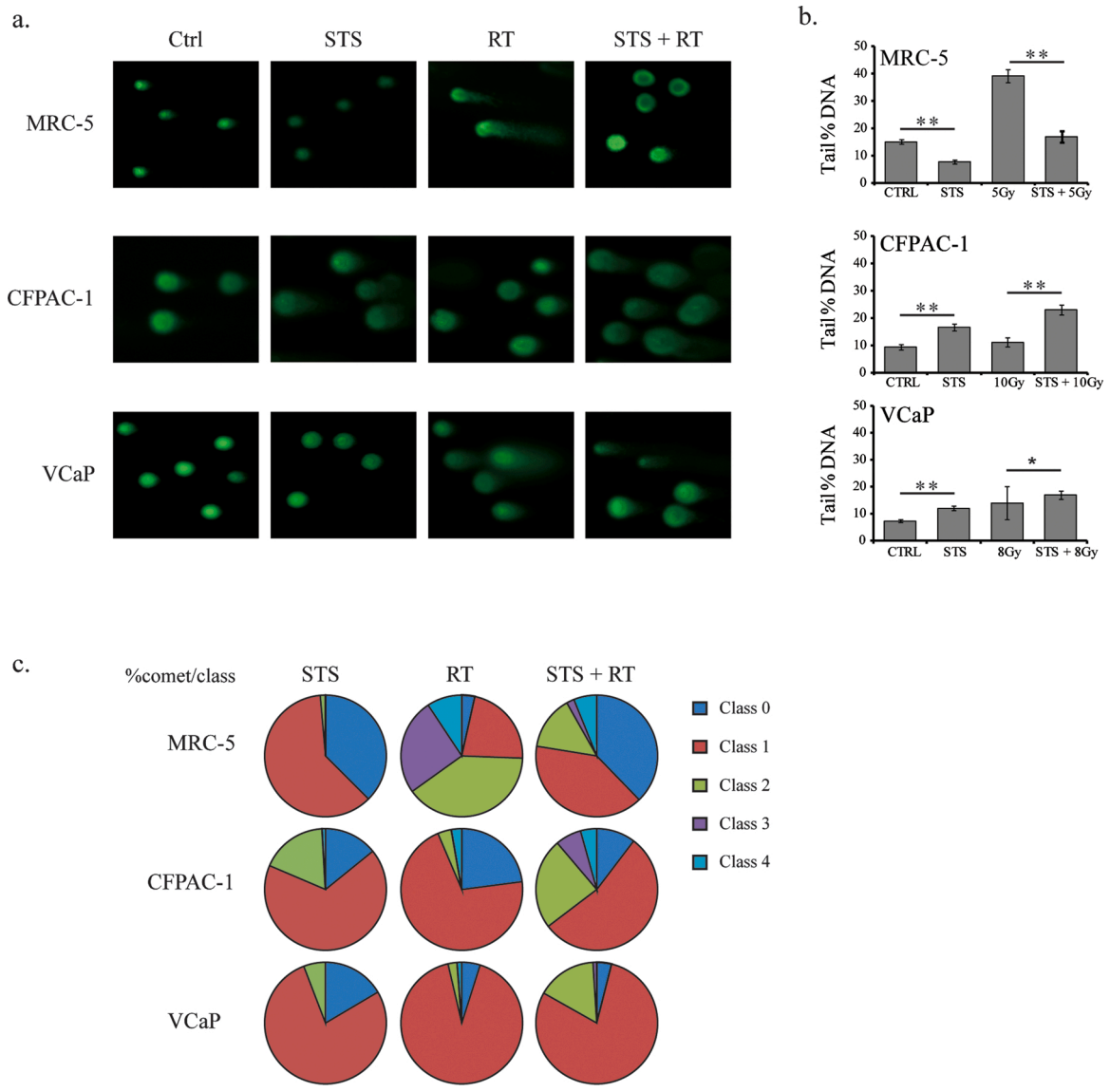

Fig. 3. DNA damage measured by alkaline comet assay. (a) Representative photomicrographs of comet assay showing cell lines stained with SBYR green after RT alone and RT combined with STS, 10x magnification. (b) DNA damage expressed as % tail DNA. Error bars represent mean ± SE. Statistical significance $*p < 0{\cdot}05$, $**p < 0{\cdot}01$. (c) Comets were categorized into 5 classes, from grade 0 - 4, according to % tail DNA. The grading was as follows: grade 0: 0 - 5, grade 1: ≥5 -25; grade 2: ≥25 -45; grade 3: ≥45 -70, grade 4: ≥70. The comparison between RT alone and RT in association with STS is the frequency of each comet class/100 comets analyzed.

evaluate the expression of glucose transporter GLUT1, which is one of the most important proteins for the uptake of glucose from the surrounding medium into the cell. GLUT1 expression was not significantly different in any cell line 72 h after RT alone but was substantially affected by STS after 4 h in both metastatic cancer cell lines (Fig. 5).

To investigate the potential synergic role of STS in association with RT, we analyzed mRNA expression of PARP1 (responsible for repairing single-strand breaks) and BRCA1 (component of homologous recombination repair system) genes. A significant decrease in BRCA1 and PARP1 expression was observed after 4 h when RT was preceded by STS in the normal cell line, MRC-5 (Fig. 5a). Conversely, both repair DNA genes were activated in CFPAC-1 cell line after RT, a significantly higher expression observed after RT + STS than RT alone. Furthermore, the fact that high BRCA1 expression was maintained after 72 h supports previous data on DNA damage and confirms that CFPAC-1 line was more sensitive to RT than the other 2 cell lines (Fig. 5b). Conversely, the modulation of DNA damage gene expression was not significant in VCaP cell lines, with the exception of PARP-1 at 4 h (Fig. 5c).

3.5. *Effect of STS on cell cycle and glucose uptake*

To investigate the effect of STS on cell cycle, we incubated MRC-5, CFPAC-1 and VCaP cell lines in STS medium (0·5 g/L glucose + 1% FBS) or in CM (1 g/L glucose + 10 % FBS) for 24 h, after which cell cycle distribution was analyzed by flow cytometry. STS substantially disrupted cell cycle distribution in MRC-5 fibroblast cell line. A 20 % increase in cells in G0/G1 phase was observed in STS-MRC-5 with a concomitant reduction in S-phase and G2/M phase cell percentages (73 % and 29 %, respectively) with respect to CTRL-MRC-5 (Fig. 6a). With regard to the tumor cell lines, nutrient depletion brought about a moderate change in CFPAC-1 cell cycle distribution with a 12 %accumulation of cells in G0/G1 phase accompanied by a 11 % loss in S-phase and a 19 % loss in G2/M phase. The histogram plot of the VCaP cell cycle showed a 12 % increase in G0/G1 phase cells, a 32 % decrease in S-phase and a 13 % decrease in G2/M cells with respect to CTRL-VCaP (Fig. 6b–c). Furthermore, glucose uptake cell capacity was measured after 24 h of STS, results indicating that, as cell viability decreased in

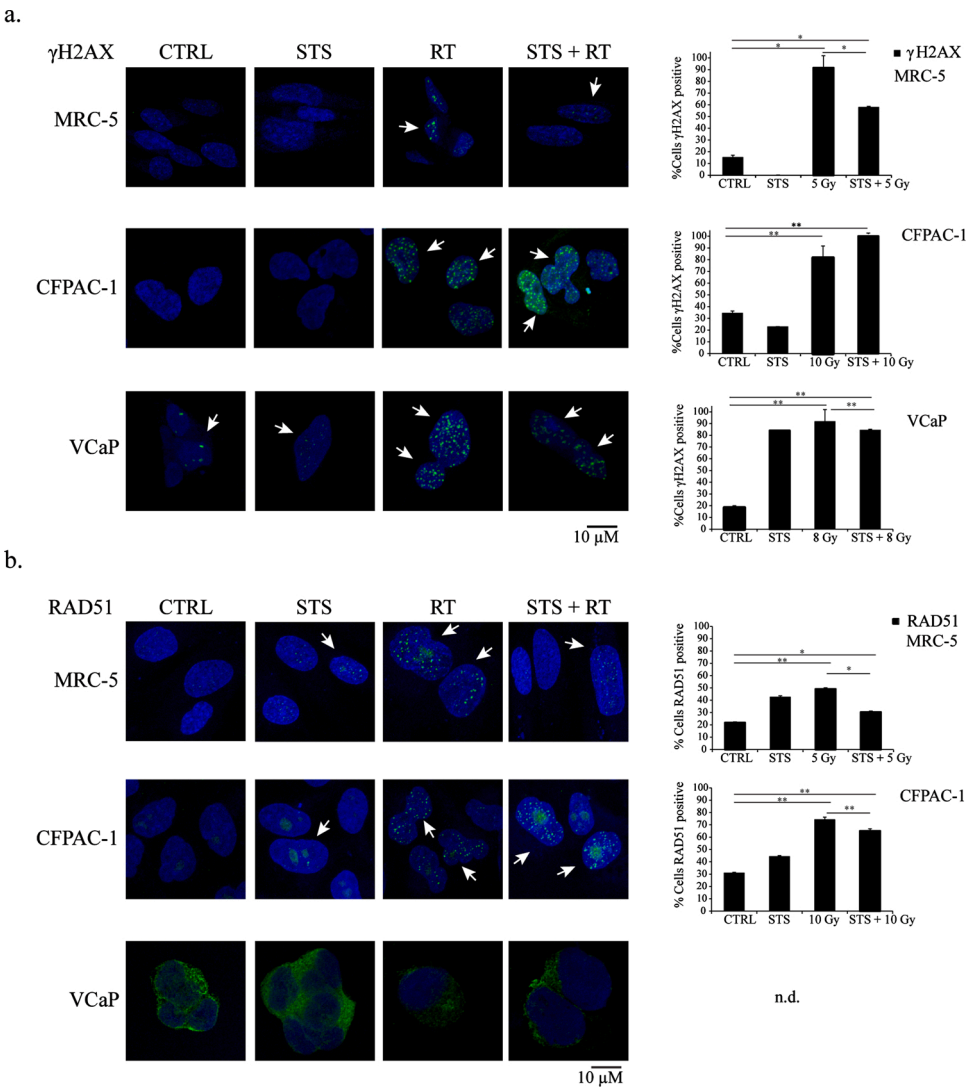

Fig. 4. Imaging quantification of γH2AX and Rad51 foci. (a, b) Micrographs of γH2AX-foci and Rad51-foci in MRC-5, CFPAC-1 and VCaP. Cell lines were cultured on coverslips in control medium (CM) or short-term starvation medium (STS) for 24 h, treated with RT alone and then stained after 72 h. At least 100 cells were scored for each condition. The percentage of positive cells was calculated for (c) γH2AX-foci and (d) for RAD51-foci. Statistical significance $*p < 0{\cdot}05$, $**p < 0{\cdot}01$.

metastatic cells, glucose uptake activity increased in CFPAC1 and keep costant in VCaP cell ines. In contrast, MRC-5 normal fibroblast cell viability was not influenced by nutrient depletion but exhibited lower overall glucose incorporation than cells in control medium (Fig. 6d–f). The highest glucose uptake capacity was observed in metastatic pancreatic cancer cells.

3.6. STS implication on tumor microenvironment

To study how starvation and its combination with radiotherapy influence angiogenesis, we exposed HUVEC cell lines, cultured in CM and STS medium, at different irradiation doses.

As shown in Fig. 7a, HUVEC cells are extremely sensitive to STS with a decrease of cell viability of about 90 % up to 72 h. Unexpectedly, STS alone significantly reduced cell viability compared to RT alone, making it difficult to assess the additional effect of pre-STS-treatment (Fig.1Sb).

In parallel, we examined the impact of STS and RT treatment on the cell ability to form three dimensional tube-like structure *in vitro*.

After 12 days, starved HUVEC cells were able to re-form branches, nodes, and meshes showing the ability to create an intense vasculature similar to control. On the contrary, starved irradiated HUVEC cells failed to form tube-like structures respect to RT alone. In particular, the combination of STS and 5 Gy caused a reduction of 26 % in branches formation, 58 % in nodes number, and 75 % in meshes number compared to RT alone. Furthermore, we observed a total loss of cell ability to form tube-like structure in the combination treatment with respect to 8 Gy alone (Fig. 7b–c).

Our results indicate that 24 h starvation suppresses endothelial cell proliferation and inhibits angiogenesis *in vitro*. Therefore, starvation my represent an external advantageous stimulus to modulate tumor angiogenesis.

To further study changes in tumor microenvironment, we characterized THP-1 cells after exposure to STS and RT treatment. We evaluated cell viability after 72 h to verify starvation and radiation sensibility. As shown in Fig. 8a STS caused 40 % of cell death in THP-1 cells, and increased cell death of 20 % in irradiated cells.

The amount of DNA damage in THP-1 cells increased in a dose-dependent manner. Comparing the % tail DNA between irradiated cells and the comet classes, we observed a mild increase in DNA damage in starved THP1 cells, except for 8 Gy doses (Fig. 8b–d). Using the THP-1 model we compared the transcriptional changes between M1 or M2 genes after RT and STS + RT (Fig. 8e). The results showed that STS combined with RT increased the expression of IL-1β in all doses tested, IL-6 in 5 Gy and 10 Gy doses, and of PPARα in 8 Gy dose. In contrast, the

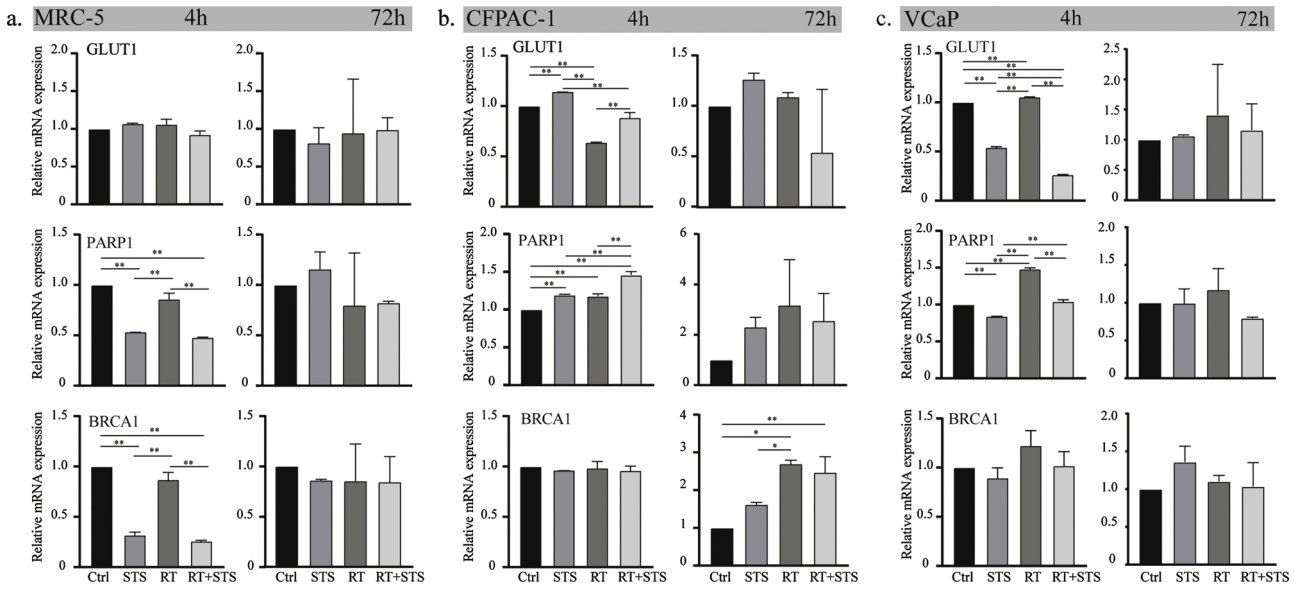

Fig. 5. Effects of radiation on mRNA expression. mRNA was isolated 4 and 72 h after RT. GLUT-1, PARP-1 and BRCA-1 gene expression was determined using quantitative real-time RT-PCR. Error bars represent the SD of three independent experiments. Statistical one-way ANOVA was used to test for differences in 4 groups. *p < 0·05, **p<0·01.

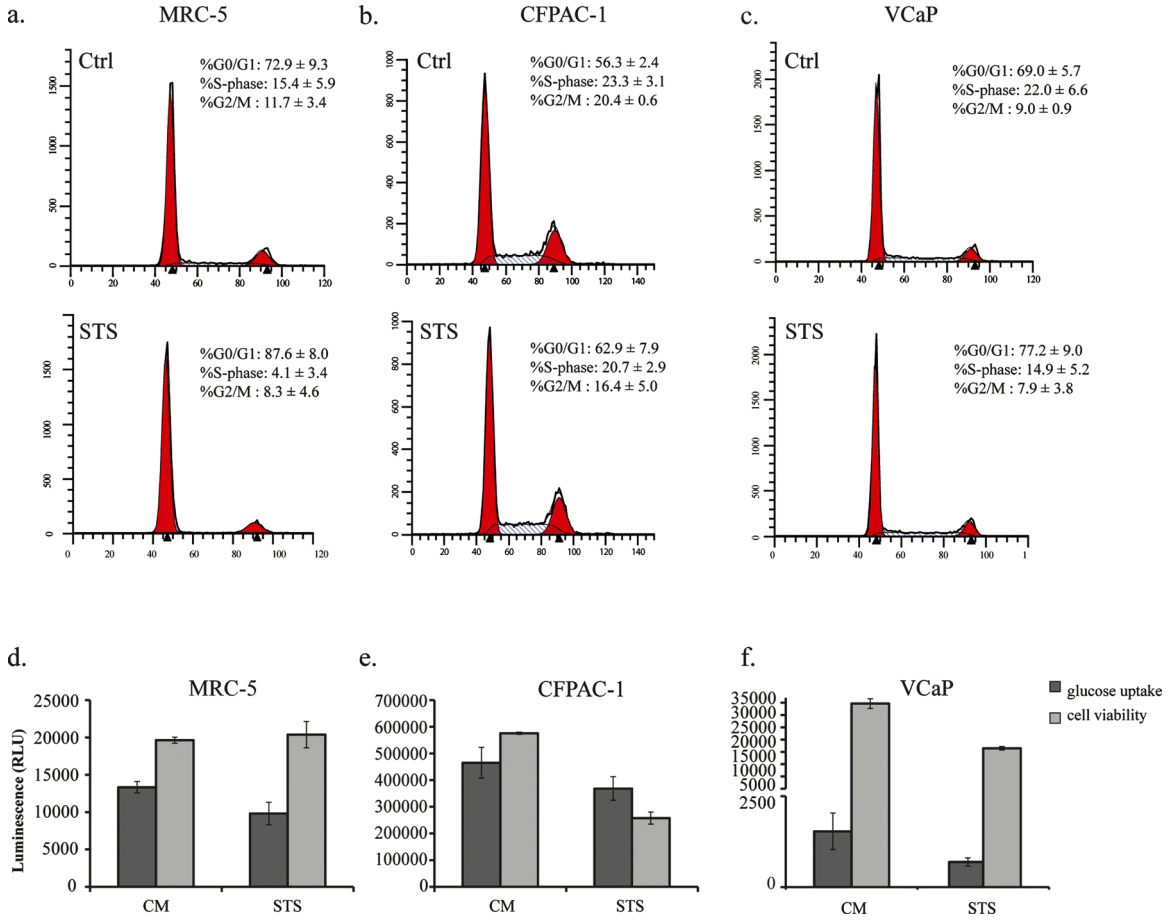

Fig. 6. Cell cycle distribution after 24 h **of STS.** (a-c) Representative cell cycle distribution in control cells and in starved cell lines (STS). Data are presented as distribution of cell populations in each phase of the cell cycle. (d-f) Effect of STS on glucose uptake in normal fibroblast and in cancer cell lines, CFPAC1 and VCaP. Cells were incubated in CM or STS medium for 24 h before assaying glucose uptake. The data are reported as the mean values (±SD) from three independent experiments.

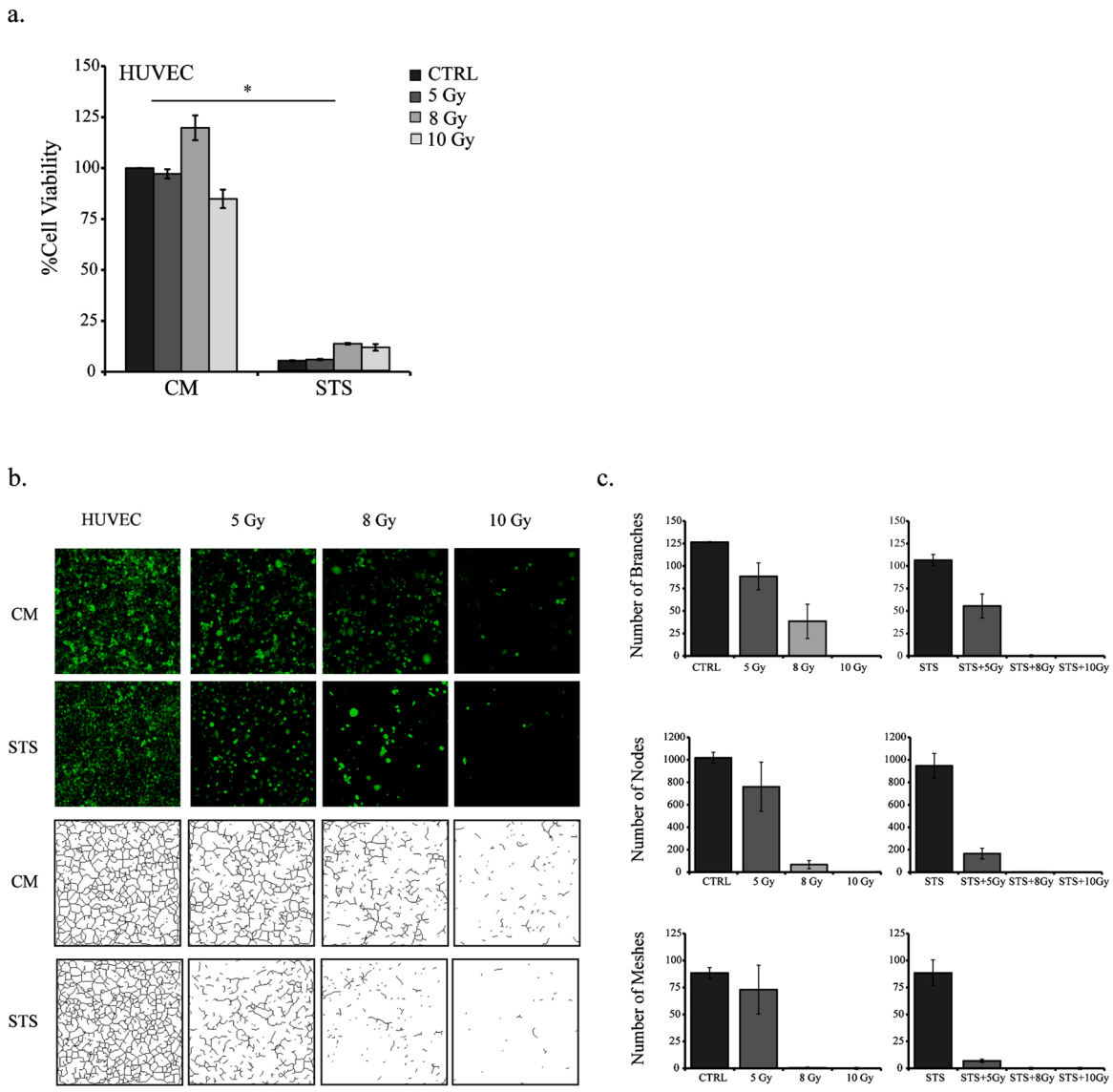

Fig. 7. Tube-like structure formation assay. (a) HUVEC cell line was exposed to ionizing radiation (IR) in normal medium (CM) or in short-term starvation medium (STS). Cell viability was evaluated using the CellTiter-Glo™ assay 72- hour after the end of IR. Data are reported as the mean ± SD for three separate experiments performed in octuplicate. (*$p < 0{\cdot}05$). (b-c) Representative images of tube-like structure formation assay and representative tree map images. Numbers of branches, nodes and meshes were measuring using Angiogenesis Analyzer plugin in ImageJ. Data are reported as the mean ± SD for three separate experiments.

M2 expression panel was not significantly affected, except for STAT6 markers, in 8 Gy treatment.

4. Discussion

Fasting, calorie restriction, and fasting-mimicking diets have become hotly-debated topics in the field of cancer, and their impact on the media, public opinion and marketing has led to much speculation and disinformation. There is evidence that nutritional support improves quality of life and survival in cancer patients [26,27]. Results from recent *in vivo* and *in vitro* studies suggest that short-term starvation (STS) or prolonged fasting (PF) may improve the efficacy of chemotherapy in some types of cancer and protect normal tissue against chemotoxicity [28,29]. Furthermore, a short-term starvation regime of 24 h not caused severe physiological implication as prolonged fasting ranging from days to weeks, in which metabolic switch, occurred after the glycogen depletion in hepatocytes, determined a dramatic body mass loss, accompanied by heart, liver and kidney loss function [30,31]. However, there are very few data available on the effect of STS used in association with RT [32]. This lack, probably, is due to the complication to combine patients diets and radiotherapy treatment, and consequently to plan a rigorous clinical trial. More preclinical research is thus needed to identify the tumor types, disease stages, and treatments that can truly benefit from dietary approaches [33,34]. We thus decided to focus on a selected metastatic cancer cell lines in which high-dose single-fraction radiotherapy could be a treatment opportunity in association with a fasting period of 24 h before radiotherapy. The selection of doses and fractionation in the metastatic setting, depends on tumor type, on the organ in which metastasis is occurred, and on patient status (*i.e.* estimated prognosis, comorbidities, acute toxicities, performance status, and systemic therapy) [35–38]. Keeping in mind the goal to recreate *in vitro* clinical tumor conditions, we thus decided to apply different radiotherapy plans, currently used by physicians, on the bases of the specific metastatic desease setting and on the organ site.

RT inhibits cell proliferation, promotes apoptosis *in vitro* and inhibits tumor growth *in vivo*, inducing single-strand (SSB) or double-strand (DSB) DNA breaks. The maintenance of genetic stability is essential for organism survival. A specialized repair system has thus been

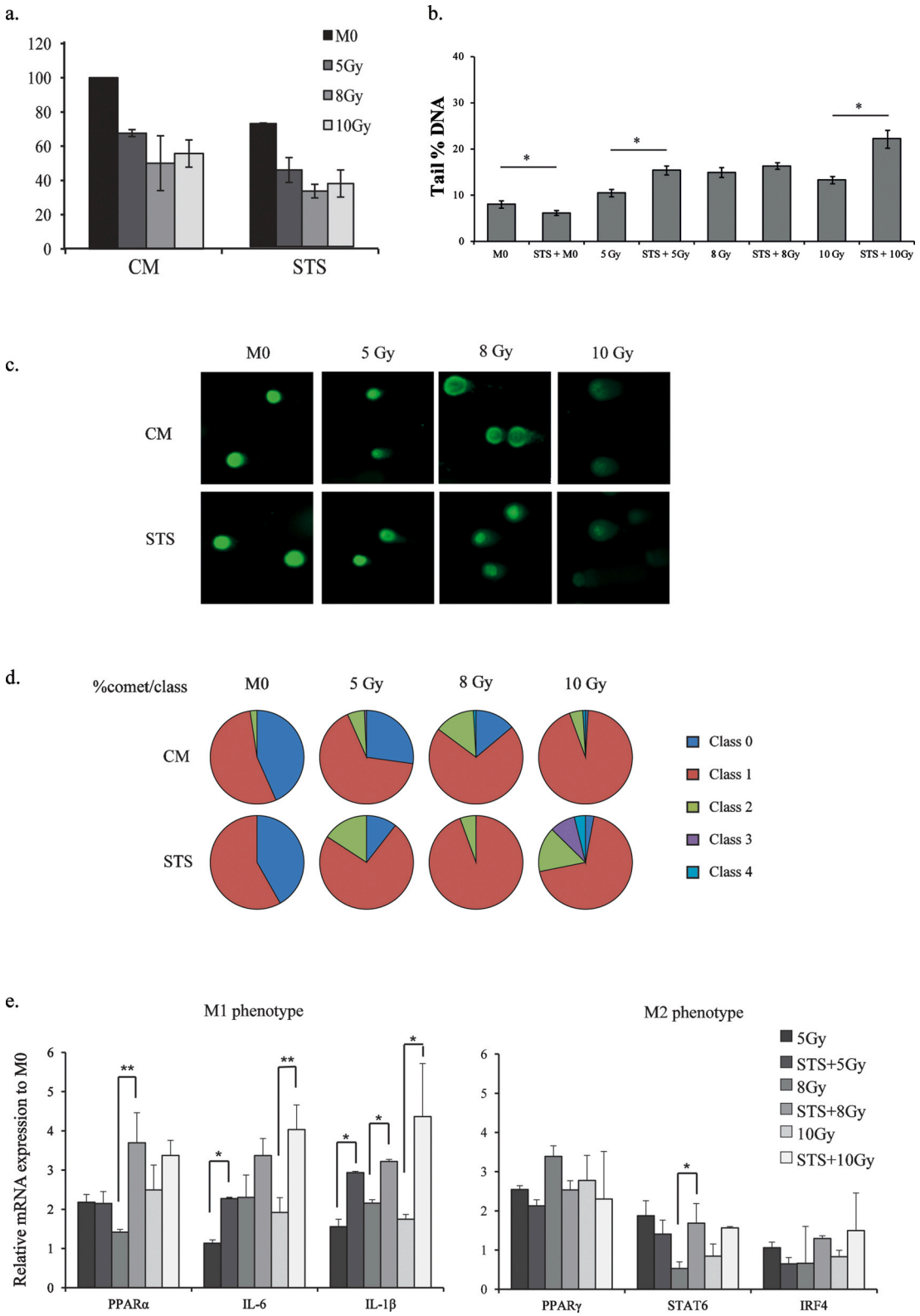

Fig. 8. STS implication on tumor microenvironment. (a) THP1 cell line was exposed to ionizing radiation in control medium (CM) or in short-term starvation medium (STS). Cell viability was evaluated using the CellTiter-Glo™ assay 72 h after the end of IR. Data are reported as the mean ± SD for three separate experiments performed in octuplicate. (b) Representative photomicrographs of comet assay showing THP1 cells stained with SBYR green after RT alone and RT combined with STS, 10x magnification. (b) DNA damage expressed as % tail DNA. Error bars represent mean ± SE. Statistical significance $*p < 0{\cdot}05$, $**p < 0{\cdot}01$. (c) Comets were categorized into 5 classes, from grade 0 - 4, according to % tail DNA. The grading was as follows: grade 0: 0 - 5, grade 1: ≥5 -25; grade 2: ≥25 -45; grade 3: ≥45 -70, grade 4: ≥70. The comparison between RT alone and RT in association with STS is the frequency of each comet class/100 comets analyzed. (d) M1 and M2 macrophages polarization gene expression panel was determined using quantitative real-time RT-PCR. THP-1 differentiated M0 macrophages were cultivated in CM or STS medium and irradiated at 5Gy, 8Gy and 10 Gy. Error bars represent the SD of three independent experiments. Statistical significance $*p < 0{\cdot}05$, $**p < 0{\cdot}01$.

developed by cells and organisms to protect DNA from endogenous and exogenous agents (*e.g.* chemicals, UV, ionizing radiation) [39]. The efficiency of DNA repair machinery, which is composed of several processes, is dependent on precise control points coordinated by DNA damage sensors and effectors proteins and on the repair system chosen based on the type of DNA lesion and the current cell cycle phase [40,41]. In oncology, this has led to the development of checkpoint inhibitors that do not directly induce DNA breaks but are used as adjuvants to DNA-damaging agents, improving their therapeutic effect [42,43].

The modification of a metabolic pathway, such as a diet intervention, which coordinates the signals between the complex cellular processes of DNA repair machinery and cell cycle, could be used to induce a temporary cell-cycle arrest to preserve genome integrity or to enhance the therapeutic efficacy of radiation. Consequently, the differential cell cycle arrest resulting from starvation or fasting could theoretically be a promising adjuvant for RT. We thus hypothesized a protective G1 and G2/M cell cycle phase arrest and used an *in vitro* model to explore the potential vulnerability of cancer cells to RT following nutrient deprivation.

Our data showed that STS for 24 h caused cell cycle perturbation, leading to a shift into G0/G1 cell cycle phase in normal fibroblasts and associated with a strong reduction in S-phase and G2/M. Conversely, this phenomenon was less evident in metastatic cancer cells. The entry of virtually all normal cells into a high-protection cell cycle arrest in response to STS may thus reduce radiation-induced DNA damage. Using the gold standard clonogenic assay [33], we observed that metastatic cancer cells became more sensitive to RT in nutrient-depleted medium, leading to a drastic reduction in their colony-forming growth. Conversely, the capacity to produce colonies was retained by normal fibroblast cells and boosted when RT was associated with STS.

Previous studies have highlighted an increase in glucose consumption by tumor cells after irradiation [44] due to the high energy demand required for DSB repair processes. It has been seen that tumor cells, which have a small intracellular amount of adenosine triphosphate (ATP), are dependent on glucose supply to induce chromatin relaxation by radiation-induced histone H3- and H4-acetylation and, consequently, to repair DNA DSBs. Conversely, normal fibroblasts are characterized by high intracellular ATP levels, which makes them resistant to the effects of glucose starvation [45,46].

Given the above premises, we hypothesized that STS may protect normal cells by regulating cell cycle and, in part, by influencing the activation of DNA repair machinery, and proceeded to measure DNA damage. Comet assay results revealed an increase in DNA damage in starved-irradiated cancer cell lines and a reduction in starved-irradiated non-tumor cells, suggesting a role of STS in regulating the DNA repair pathway. We also observed an accumulation of nuclear γH2AX in metastatic cancer cells that correlated with the damaged comet class.

Several studies have reported the association of H2AX phosphorylation with the induction DSBs after IR or other DNA-damaging agents, and also with DNA replication stress [47–50]. Given the evidence of increased DNA damage in comet assay in starved metastatic cells, we investigated the changes in H2AX phosphorylation in such cells during replication stress. Here we have shown a moderate increase in H2AX positive cells in starved tumor cells, indicating that measured DNA damage could be in part due to replication stress.

Moreover, our results showed that the expression of RAD51 is both nuclear and cytoplasmic, and it varies among cell lines. CFPAC-1 shown an accumulation of nuclear RAD51 in response to irradiation damage, while VCaP cell lines are characterized by high cytoplasmic RAD51 expression levels. Recent data demonstrate a possible correlation with cytoplasm RAD51 protein expression and tumor aggressivity especially in prostate and breast cancers suggesting that RAD51 might have diagnostic value [51,52]. Furthermore, our DNA damage measurement provided a potentially useful molecular method for predicting treatment outcome by correlating γH2AX and RAD51 foci count and comet damage classification.

Nutrient levels, such as glucose, may generate a protective environment that reduces DNA damage in healthy cells and, at the same time, create hostile conditions for tumor cells. It is well known that cancer cells are addicted to glucose as a source of energy, favoring glycolysis in aerobic conditions, a phenomenon known as the "Warburg effect" [53]. Others studies [54,55]) using a glucose analog to inhibit the glycolytic pathway also reported an increase in radiation-induced damage. This may explain why different starved cells (normal and tumor) contribute in different ways to the response of DNA damage. However, further research is needed to better understand metabolic alterations and pathway regulation caused by starvation.

GLUT1 is a member of glucose membrane transporters whose overexpression in cancer is frequently associated with chemoresistance. Several studies have shown that the reduction of glucose and IGF-1 and the inhibition of mTOR pathway modulate the response to chemotherapy *in vitro* in cancer cells [2,10].

We observed that a 24 -h STS modulated GLUT-1 expression in metastatic cancer cell lines, suggesting that glucose is the preferred fuel for tumor and that metastatic cancer cells are susceptible to changes in glucose levels. We would therefore expect glucose transport to be closely regulated by glucose availability [56].

In our study, metabolic changes led to a modification of PARP-1 and BRCA-1 gene expression. PARP-1, a protein involved in the repair of SSBs, and BRCA-1, an important component of the HR pathway, play an important role in DNA repair pathways, transcriptional regulation, cell death, angiogenesis, and metabolism [57,58]. The increase in PARP-1 and BRCA-1 gene expression in pancreatic cell lines, and the abnormalities in cell cycle after STS and RT underlined the sensitivity of CFPAC-1 to this combination. The decline in PARP-1 and BRCA-1 gene expression and the DNA damage observed in non-tumor cells indicated a protective role of STS.

Given the results obtained, we examined the potential role of STS in the modulation of tumor microenvironment, including endothelial compartment and immune cells. Angiogenesis is a highly regulated process exploited by tumor cells to ensure a constant nutrients supply to sustain their growth and to provide the necessary vasculature needed for metastasis spreading. During angiogenesis, vascular endothelial cells respond to various factors and signal that may promote or inhibit angiogenic process [59,60]. Previous studies have highlighted how high level of glucose in diabetic may contribute to excessive angiogenesis contributing to disease complications such as retinopathy, nephropathy and cardiovascular disease [61]. In our study, STS led to a reduction of endothelial cell viability, resulting in a marked disruption of tube-like structure formation *in vitro* on starved- irradiated endothelial cells. These data highlighted further antitumor properties of STS that resulted able to decrease the fuel (nutrient and oxygen) supply to tumor cells.

Macrophages are the most important cells of innate immune system, and are involved in the regulation of host defense, inflammation and cancer. Due to their transcriptional plasticity, they can change the profile depending on tumor microenvironment. Recent studied indicate that nutrients modulation could have a potent effect on monocytes and on both B and T cells depending by fasting duration and severity, determining opposite effects on the number and function of immune cells [62–65]. In tumor microenvironment, macrophages have two states of polarization M1-cancer inhibiting and M2 cancer promoting. M2-like macrophage support almost all hallmarks of cancer by producing growth factors, cytokine, remodeling extracellular matrix, promoting angiogenesis and migration, suppressing anti-tumor immunity.

We found that short-term starvation modified gene expression pattern suggesting an *in vitro* mitigation of cancer chronic inflammation. Altogether, these data showed how nutrient modulation could be a critical regulator of tumor microenvironment.

In conclusion, our findings indicate that glucose starvation impaired the repair of radiation-induced DNA DSBs, increasing the radiosensitivity of metastatic tumor cells, but did not affect the response of normal fibroblasts to RT. Furthermore, the assessment of DNA damage in

peripheral blood mononuclear cells (PBMCs) of patients under nutrient modulation, using comet assay tools or H2AX phosphorylation, could serve to evaluate susceptibility to radiotherapy in support of clinical studies. The data obtained on the combined use of STS and RT, also provide a potentially scientific rationale for further preclinical and clinical studies. However, further evidence is needed of the physiological safety and feasibility of our *in vitro* model before it can implemented in a clinical setting.

Funding sources

No funding was received.

Transparency document

The Transparency document associated with this article can be found in the online version.

Transparency document.

CRediT authorship contribution statement

Sara Pignatta: Conceptualization, Validation, Investigation, Resources, Writing - original draft, Writing - review & editing, Visualization. **Michela Cortesi:** Writing - original draft, Writing - review & editing. **Chiara Arienti:** Validation, Data curation. **Michele Zanoni:** Investigation. **Claudia Cocchi:** Investigation. **Anna Sarnelli:** Formal analysis. **Donatella Arpa:** Methodology. **Filippo Piccinini:** Software. **Anna Tesei:** Supervision, Conceptualization, Writing - original draft.

Declaration of Competing Interest

The authors report no declarations of interest.

Acknowledgements

We thank Loris Zamai (University of Urbino “Carlo Bo”, Italy) for scientific support and Gráinne Tierney (Istituto Scientifico Romagnolo per lo Studio e la Cura dei Tumori (IRST) IRCCS) for editorial assistance.

Appendix A. Supplementary data

Supplementary material related to this article can be found, in the online version, at doi:https://doi.org/10.1016/j.dnarep.2020.102949.

References

[1] T. Bortfeld, R. Jeraj, The physical basis and future of radiation therapy, Br. J. Radiol. 84 (2011) 485–498, https://doi.org/10.1259/bjr/86221320.
[2] S. Brandhorst, M. Wei, S. Hwang, T.E. Morgan, V.D. Longo, Short-term calorie and protein restriction provide partial protection from chemotoxicity but do not delay glioma progression, Exp. Gerontol. 48 (2013) 1120–1128, https://doi.org/10.1016/j.exger.2013.02.016.
[3] T.A.C. Kennedy, M.T. Corkum, A.V. Louie, Stereotactic radiotherapy in oligometastatic cancer, Chinese Clin. Oncol. 6 (2017), https://doi.org/10.21037/cco.2017.06.20.
[4] S. Otake, T. Goto, Cancers Stereotactic Radiotherapy for Oligometastasis (n.d.), 2020, https://doi.org/10.3390/cancers11020133.
[5] D. Lettieri-Barbato, K. Aquilano, Pushing the limits of cancer therapy: the nutrient game, Front. Oncol. 8 (2018) 148, https://doi.org/10.3389/fonc.2018.00148.
[6] T.L. Jensen, M.K. Kiersgaard, D.B. Sørensen, L.F. Mikkelsen, Fasting of mice: a review, Lab. Anim. 47 (2013) 225–240, https://doi.org/10.1177/0023677213501659.
[7] K.L. Tinkum, K.M. Stemler, L.S. White, A.J. Loza, S. Jeter-Jones, B.M. Michalski, C. Kuzmicki, R. Pless, T.S. Stappenbeck, D. Piwnica-Worms, H. Piwnica-Worms, Fasting protects mice from lethal DNA damage by promoting small intestinal epithelial stem cell survival, Proc. Natl. Acad. Sci. U. S. A. 112 (2015) E7148–E7154, https://doi.org/10.1073/pnas.1509249112.
[8] S. de Groot, M.P.G. Vreeswijk, M.J.P. Welters, G. Gravesteijn, J.J.W.A. Boei, A. Jochems, D. Houtsma, H. Putter, J.J.M. van der Hoeven, J.W.R. Nortier, H. Pijl, J.R. Kroep, The effects of short-term fasting on quality of life and tolerance to chemotherapy in patients with breast and ovarian cancer: a randomized cross-over pilot study, BMC Cancer 15 (2015) 1–10, https://doi.org/10.1186/s12885-015-1663-5.
[9] R.J. Klement, Fasting, fats, and physics: combining ketogenic and radiation therapy against cancer, Complement. Med. Res. 25 (2018) 102–113, https://doi.org/10.1159/000484045.
[10] F. Safdie, S. Brandhorst, M. Wei, W. Wang, C. Lee, S. Hwang, P.S. Conti, T.C. Chen, V.D. Longo, Fasting enhances the response of glioma to chemo- and radiotherapy, PLoS One 7 (2012), https://doi.org/10.1371/journal.pone.0044603 e44603.
[11] C. Lee, V.D. Longo, Fasting vs dietary restriction in cellular protection and cancer treatment: from model organisms to patients, Oncogene 30 (2011) 3305–3316, https://doi.org/10.1038/onc.2011.91.
[12] L. Raffaghello, C. Lee, F.M. Safdie, M. Wei, F. Madia, G. Bianchi, V.D. Longo, Starvation-dependent differential stress resistance protects normal but not cancer cells against high-dose chemotherapy, Proc. Natl. Acad. Sci. U. S. A. 105 (2008) 8215–8220, https://doi.org/10.1073/pnas.0708100105.
[13] D. Hanahan, R.A. Weinberg, Hallmarks of cancer: the next generation, Cell 144 (2011) 646–674, https://doi.org/10.1016/j.cell.2011.02.013.
[14] R. Buono, V.D. Longo, Starvation, stress resistance, and cancer, Trends Endocrinol. Metab. 29 (2018) 271–280, https://doi.org/10.1016/j.tem.2018.01.008.
[15] C.V. Dang, A. Le, P. Gao, MYC-induced cancer cell energy metabolism and therapeutic opportunities, Clin. Cancer Res. 15 (2009) 6479–6483, https://doi.org/10.1158/1078-0432.CCR-09-0889.
[16] S. Zhang, D. Yu, PI(3)king apart PTEN's role in cancer, Clin. Cancer Res. 16 (2010) 4325–4330, https://doi.org/10.1158/1078-0432.CCR-09-2990.
[17] G. Bianchi, R. Martella, S. Ravera, C. Marini, S. Capitanio, A. Orengo, L. Emionite, C. Lavarello, A. Amaro, A. Petretto, U. Pfeffer, G. Sambuceti, V. Pistoia, L. Raffaghello, V.D. Longo, Fasting induces anti-Warburg effect that increases respiration but reduces ATP-synthesis to promote apoptosis in colon cancer models, Oncotarget 6 (2015) 11806–11819, https://doi.org/10.18632/oncotarget.3688.
[18] Y. Shi, E. Felley-Bosco, T.M. Marti, K. Orlowski, M. Pruschy, R.A. Stahel, Starvation-induced activation of ATM/Chk2/p53 signaling sensitizes cancer cells to cisplatin, BMC Cancer 12 (2012) 571, https://doi.org/10.1186/1471-2407-12-571.
[19] K.J. Williams, B.A. Telfer, R.E. Airley, H.P.W. Peters, M.R. Sheridan, A.J. Van der Kogel, A.L. Harris, I.J. Stratford, A protective role for HIF-1 in response to redox manipulation and glucose deprivation: implications for tumorigenesis, Oncogene 21 (2002) 282–290, https://doi.org/10.1038/sj.onc.1205047.
[20] E. Moreno Roig, A. Groot, A. Yaromina, T. Hendrickx, L. Barbeau, L. Giuranno, G. Dams, J. Ient, V. Olivo Pimentel, M. van Gisbergen, L. Dubois, M. Vooijs, HIF-1α and HIF-2α differently regulate the radiation sensitivity of NSCLC cells, Cells 8 (2019) 45, https://doi.org/10.3390/cells8010045.
[21] A. Tesei, A. Sarnelli, C. Arienti, E. Menghi, L. Medri, E. Gabucci, S. Pignatta, M. Falconi, R. Silvestrini, W. Zoli, V. D'Errico, A. Romeo, E. Parisi, R. Polico, In vitro irradiation system for radiobiological experiments, Radiat. Oncol. 8 (2013) 257, https://doi.org/10.1186/1748-717X-8-257.
[22] C. Arienti, M. Zanoni, S. Pignatta, A. Del Rio, S. Carloni, M. Tebaldi, G. Tedaldi, A. Tesei, Preclinical evidence of multiple mechanisms underlying trastuzumab resistance in gastric cancer, Oncotarget 7 (2016) 18424–18439, https://doi.org/10.18632/oncotarget.7575.
[23] A. Tesei, G. Brigliadori, S. Carloni, F. Fabbri, P. Ulivi, C. Arienti, A. Sparatore, P. Del Soldato, A. Pasini, D. Amadori, R. Silvestrini, W. Zoli, Organosulfur derivatives of the HDAC inhibitor valproic acid sensitize human lung cancer cell lines to apoptosis and to cisplatin cytotoxicity, J. Cell. Physiol. 227 (2012) 3389–3396, https://doi.org/10.1002/jcp.24039.
[24] Nobuyuki Otsu, A threshold selection method from gray-level histograms, IEEE Trans. Syst. Man Cybern. 9 (1979) 62–66.
[25] B.M. Gyori, G. Venkatachalam, P.S. Thiagarajan, D. Hsu, M.V. Clement, OpenComet: an automated tool for comet assay image analysis, Redox Biol. 2 (2014) 457–465, https://doi.org/10.1016/j.redox.2013.12.020.
[26] R. Caccialanza, E. Cereda, F. De Lorenzo, G. Farina, P. Pedrazzoli, AIOM-SINPE-FAVO Working Group, to fast, or not to fast before chemotherapy, that is the question, BMC Cancer 18 (2018) 337, https://doi.org/10.1186/s12885-018-4245-5.
[27] S.P. Bauersfeld, C.S. Kessler, M. Wischnewsky, A. Jaensch, N. Steckhan, R. Stange, B. Kunz, B. Brückner, J. Sehouli, A. Michalsen, The effects of short-term fasting on quality of life and tolerance to chemotherapy in patients with breast and ovarian cancer: A randomized cross-over pilot study, BMC Cancer 18 (2018) 476, https://doi.org/10.1186/s12885-018-4353-2.
[28] F. Antunes, M. Corazzari, G. Pereira, G.M. Fimia, M. Piacentini, S. Smaili, Fasting boosts sensitivity of human skin melanoma to cisplatin-induced cell death, Biochem. Biophys. Res. Commun. 485 (2017) 16–22, https://doi.org/10.1016/j.bbrc.2016.09.149.
[29] S.A. Huisman, P. de Bruijn, I.M. Ghobadi Moghaddam-Helmantel, J.N. M. IJzermans, E.A.C. Wiemer, R.H.J. Mathijssen, R.W.F. de Bruin, Fasting protects against the side effects of irinotecan treatment but does not affect anti-tumour activity in mice, Br. J. Pharmacol. 173 (2016) 804–814, https://doi.org/10.1111/bph.13317.
[30] S.D. Anton, K. Moehl, W.T. Donahoo, K. Marosi, S.A. Lee, A.G. Mainous, C. Leeuwenburgh, M.P. Mattson, Flipping the metabolic switch: understanding and applying the health benefits of fasting, Obesity 26 (2018) 254–268, https://doi.org/10.1002/oby.22065.
[31] A. Nencioni, I. Caffa, S. Cortellino, V.D. Longo, Fasting and cancer: molecular mechanisms and clinical application, Nat. Rev. Cancer 18 (2018) 707–719, https://doi.org/10.1038/s41568-018-0061-0.

[32] B.A. Simone, T. Dan, A. Palagani, L. Jin, S.Y. Han, C. Wright, J.E. Savage, R. Gitman, M.K. Lim, J. Palazzo, M.P. Mehta, N.L. Simone, Caloric restriction coupled with radiation decreases metastatic burden in triple negative breast cancer, Cell Cycle 15 (2016) 2265–2274, https://doi.org/10.1080/15384101.2016.1160982.
[33] A.L. Dunne, M.E. Price, C. Mothersill, S.R. McKeown, T. Robson, D.G. Hirst, Relationship between clonogenic radiosensitivity, radiation-induced apoptosis and DNA damage/repair in human colon cancer cells, Br. J. Cancer 89 (2003) 2277–2283, https://doi.org/10.1038/sj.bjc.6601427.
[34] N. Feofanova, J.M. Geraldo, L.M. De Andrade, Radiation oncology in vitro: trends to improve radiotherapy through molecular targets, Biomed Res. Int. 2014 (2014), https://doi.org/10.1155/2014/461687.
[35] F. De Felice, A. Piccioli, D. Musio, V. Tombolini, The role of radiation therapy in bone metastases management, Oncotarget 8 (2017) 25691–25699, https://doi.org/10.18632/oncotarget.14823.
[36] A.A. Butala, S.S. Lo, J.A. Jones, Advanced radiotherapy for metastatic disease—a major stride or a futile effort? Ann. Palliat. Med. 8 (2019) 337–351, https://doi.org/10.21037/apm.2019.07.07.
[37] A.M. Romero, W. Wunderink, S.M. Hussain, J.A. De Pooter, B.J.M. Heijmen, P.C.J. M. Nowak, J.J. Nuyttens, R.P. Brandwijk, C. Verhoef, J.N.M. Ijzermans, P. C. Levendag, Stereotactic body radiation therapy for primary and metastatic liver tumors: a single institution phase i-ii study, Acta Oncol. (Madr)., Acta Oncol (2006) 831–837, https://doi.org/10.1080/02841860600897934.
[38] T.E. Schefter, K.E. Rusthoven, B.D. Kavanagh, H. Cardenes, V.W. Stieber, S. H. Burri, S.J. Feigenberg, M.A. Chidel, T.J. Pugh, W. Franklin, M. Kane, L. E. Gaspar, Multi-institutional phase I/II trial of stereotactic body radiation therapy for liver metastases, J. Clin. Oncol. 27 (2009) 1572–1578, https://doi.org/10.1200/JCO.2008.19.6329.
[39] F. Dietlein, L. Thelen, H.C. Reinhardt, Cancer-specific defects in DNA repair pathways as targets for personalized therapeutic approaches, Trends Genet. 30 (2014) 326–339, https://doi.org/10.1016/j.tig.2014.06.003.
[40] J. Most, V. Tosti, L.M. Redman, L. Fontana, Calorie restriction in humans: an update, Ageing Res. Rev. 39 (2017) 36–45, https://doi.org/10.1016/j.arr.2016.08.005.
[41] T.M. Pawlik, K. Keyomarsi, Role of cell cycle in mediating sensitivity to radiotherapy, Int. J. Radiat. Oncol. Biol. Phys. 59 (2004) 928–942, https://doi.org/10.1016/j.ijrobp.2004.03.005.
[42] M. Javle, N.J. Curtin, The role of PARP in DNA repair and its therapeutic exploitation, Br. J. Cancer 105 (2011) 1114–1122, https://doi.org/10.1038/bjc.2011.382.
[43] C. Vernieri, S. Casola, M. Foiani, F. Pietrantonio, F. de Braud, V. Longo, Targeting Cancer metabolism: dietary and pharmacologic interventions, Cancer Discov. 6 (2016) 1315–1333, https://doi.org/10.1158/2159-8290.CD-16-0615.
[44] K. Dittmann, C. Mayer, H.P. Rodemann, S.M. Huber, EGFR cooperates with glucose transporter SGLT1 to enable chromatin remodeling in response to ionizing radiation, Radiother. Oncol. 107 (2013) 247–251, https://doi.org/10.1016/j.radonc.2013.03.016.
[45] R. Ampferl, H.P. Rodemann, C. Mayer, T.T.A. Höfling, K. Dittmann, Glucose starvation impairs DNA repair in tumour cells selectively by blocking histone acetylation, Radiother. Oncol. 126 (2018) 465–470, https://doi.org/10.1016/j.radonc.2017.10.020.
[46] C. Marini, G. Bianchi, A. Buschiazzo, S. Ravera, R. Martella, G. Bottoni, A. Petretto, L. Emionite, E. Monteverde, S. Capitanio, E. Inglese, M. Fabbi, F. Bongioanni, L. Garaboldi, P. Bruzzi, A.M. Orengo, L. Raffaghello, G. Sambuceti, Divergent targets of glycolysis and oxidative phosphorylation result in additive effects of metformin and starvation in colon and breast cancer, Sci. Rep. 6 (2016), https://doi.org/10.1038/srep19569.
[47] P. M, S. A, B. P, H2AX phosphorylation: its role in DNA damage response and Cancer therapy, J. Nucleic Acids 2010 (2010), https://doi.org/10.4061/2010/920161.
[48] E.M. Matthew, T.J. Yen, D.T. Dicker, J.F. Dorsey, W. Yang, A. Navaraj, W.S. El-Deiry, Replication stress, defective S-phase checkpoint and increased death in Plk2-deficient human cancer cells, Cell Cycle 6 (2007) 2571–2578, https://doi.org/10.4161/cc.6.20.5079.
[49] M.E. Gagou, P. Zuazua-Villar, M. Meuth, Enhanced H2AX phosphorylation, DNA replication fork arrest, and cell death in the absence of Chk1, Mol. Biol. Cell 21 (2010) 739–752, https://doi.org/10.1091/mbc.E09-07-0618.
[50] W.Z. Tu, B. Li, B. Huang, Y. Wang, X.D. Liu, H. Guan, S.M. Zhang, Y. Tang, W. Q. Rang, P.K. Zhou, γh2AX foci formation in the absence of DNA damage: mitotic H2AX phosphorylation is mediated by the DNA-PKcs/CHK2 pathway, FEBS Lett. 587 (2013) 3437–3443, https://doi.org/10.1016/j.febslet.2013.08.028.
[51] A. Mitra, C. Jameson, Y. Barbachano, L. Sanchez, Z. Kote-Jarai, S. Peock, N. Sodha, E. Bancroft, A. Fletcher, C. Cooper, D. Easton, R. Eeles, C.S. Foster, Overexpression of RAD51 occurs in aggressive prostatic cancer, Histopathology 55 (2009) 696–704, https://doi.org/10.1111/j.1365-2559.2009.03448.x.
[52] A.T. Alshareeda, O.H. Negm, M.A. Aleskandarany, A.R. Green, C. Nolan, P. J. TigHhe, S. Madhusudan, I.O. Ellis, E.A. Rakha, Clinical and biological significance of RAD51 expression in breast cancer: a key DNA damage response protein, Breast Cancer Res. Treat. 159 (2016) 41–53, https://doi.org/10.1007/s10549-016-3915-8.
[53] R.K. Tekade, X. Sun, The Warburg effect and glucose-derived cancer theranostics, Drug Discov. Today 22 (2017) 1637–1653, https://doi.org/10.1016/j.drudis.2017.08.003.
[54] B.K. Mohanti, G.K. Rath, N. Anantha, V. Kannan, B.S. Das, B.A. Chandramouli, A. K. Banerjee, S. Das, A. Jena, R. Ravichandran, U.P. Sahi, R. Kumar, N. Kapoor, V. K. Kalia, B.S. Dwarakanath, V. Jain, Improving cancer radiotherapy with 2-deoxy-D-glucose: phase I/II clinical trials on human cerebral gliomas, Int. J. Radiat. Oncol. Biol. Phys. 35 (1996) 103–111, https://doi.org/10.1016/s0360-3016(96)85017-6.
[55] V. Jain, S.P. Singh, S. Singh, Effects of 5-bromo-2-deoxyuridine and 2-deoxy-d-glucose on radiation-induced micronuclei in mouse bone marrow, Int. J. Radiat. Biol. 58 (1990) 791–797.
[56] A. Klip, T. Tsakiridis, A. Marette, P.A. Ortiz, Regulation of expression of glucose transporters by glucose: a review of studies in vivo and in cell cultures, FASEB J. 8 (1994) 43–53, https://doi.org/10.1096/fasebj.8.1.8299889.
[57] J. Wu, L.Y. Lu, X. Yu, The role of BRCA1 in DNA damage response, Protein Cell 1 (2010) 117–123, https://doi.org/10.1007/s13238-010-0010-5.
[58] V.J. Bhute, Y. Ma, X. Bao, S.P. Palecek, The poly (ADP-Ribose) polymerase inhibitor veliparib and radiation cause significant cell line dependent metabolic changes in breast cancer cells, Sci. Rep. 6 (2016) 36061, https://doi.org/10.1038/srep36061.
[59] D.R. Bielenberg, B.R. Zetter, The contribution of angiogenesis to the process of metastasis, Cancer J. (United States) 21 (2015) 267–273, https://doi.org/10.1097/PPO.0000000000000138.
[60] N. Nishida, H. Yano, T. Nishida, T. Kamura, M. Kojiro, Angiogenesis in cancer, Vasc. Health Risk Manage. 2 (2006) 213–219, https://doi.org/10.2147/vhrm.2006.2.3.213.
[61] R. Cheng, J. xing Ma, Angiogenesis in diabetes and obesity, Rev. Endocr. Metab. Disord. 16 (2015) 67–75, https://doi.org/10.1007/s11154-015-9310-7.
[62] S. Jordan, N. Tung, M. Casanova-Acebes, C. Chang, C. Cantoni, D. Zhang, T. H. Wirtz, S. Naik, S.A. Rose, C.N. Brocker, A. Gainullina, D. Hornburg, S. Horng, B. B. Maier, P. Cravedi, D. LeRoith, F.J. Gonzalez, F. Meissner, J. Ochando, A. Rahman, J.E. Chipuk, M.N. Artyomov, P.S. Frenette, L. Piccio, M.L. Berres, E. J. Gallagher, M. Merad, Dietary intake regulates the circulating inflammatory monocyte pool, Cell 178 (2019) 1102–1114, https://doi.org/10.1016/j.cell.2019.07.050, e17.
[63] N. Collins, S.J. Han, M. Enamorado, V.M. Link, B. Huang, E.A. Moseman, R. J. Kishton, J.P. Shannon, D. Dixit, S.R. Schwab, H.D. Hickman, N.P. Restifo, D. B. McGavern, P.L. Schwartzberg, Y. Belkaid, The bone marrow protects and optimizes immunological memory during dietary restriction, Cell 178 (2019) 1088–1101, https://doi.org/10.1016/j.cell.2019.07.049, e15.
[64] M. Nagai, R. Noguchi, D. Takahashi, T. Morikawa, K. Koshida, S. Komiyama, N. Ishihara, T. Yamada, Y.I. Kawamura, K. Muroi, K. Hattori, N. Kobayashi, Y. Fujimura, M. Hirota, R. Matsumoto, R. Aoki, M. Tamura-Nakano, M. Sugiyama, T. Katakai, S. Sato, K. Takubo, T. Dohi, K. Hase, Fasting-refeeding impacts immune cell dynamics and mucosal immune responses, Cell 178 (2019) 1072–1087, https://doi.org/10.1016/j.cell.2019.07.047, e14.
[65] N. Shanmugam, M.A. Reddy, M. Guha, R. Natarajan, High glucose-induced expression of proinflammatory cytokine and chemokine genes in monocytic cells, Diabetes 52 (2003) 1256–1264, https://doi.org/10.2337/diabetes.52.5.1256.